Materials Chemistry Horizons RESEARCH

$ZnFe_2O_4@Fe_3O_4$ Nanocatalyst for the Synthesis of the 1,8-Dioxooctahydroxanthene: Antioxidant and Antimicrobial Studies

Fatemeh Ghayem, Shefa Mirani Nezhad, Samanesadat Hosseini, Seied Ali Pourmousavi*

School of Chemistry, Damghan University, Damghan, 36716-45667

Corresponding author: pourmousavi@du.ac.ir (S.A. Pourmousavi)

Mater. Chem. Horizons, 2023, 2(3), 207-224 10.22128/mch.2023.704.1046 OPEN ACCESS

ABSTRACT

This study aims to prepare and evaluate the catalytic advantages of $ZnFe_2O_4@Fe_3O_4$ in the synthesis of 1,8-dioxo-octahydroxanthene derivatives. The catalyst was fully characterized by FTIR, EDX, XRD, FESEM, TGA, and VSM analyses. The $ZnFe_2O_4@Fe_3O_4$ was applied as a catalyst for the synthesis of 1,8-dioxo-octahydroxanthenes. The products were synthesized in significant yields (85–95%) in short reaction times (15–60 min) without laborious work-up. The biological activity of 1,8-dioxo-octahydroxant derivatives was studied. These compounds showed antioxidant activity between 64.4 and 90.2% and their antimicrobial activity against *S. enterica*, *E. coli*, *L. monocytogenes*, *S. aureus*, and *E. faecalis* was investigated.

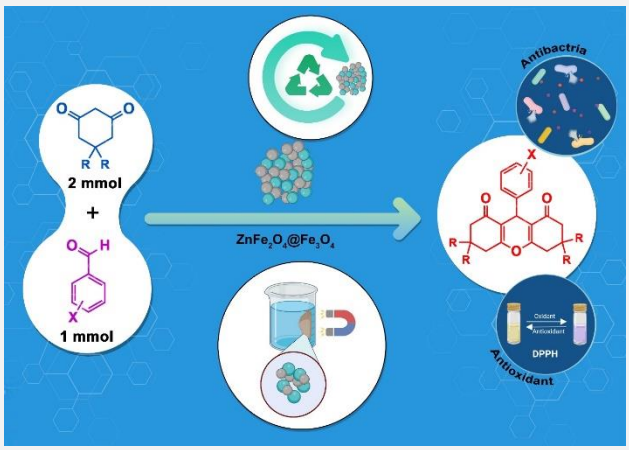

Keywords: $ZnFe_2O_4@Fe_3O_4$, composite, 1,8-dioxo-octahydroxanthene, antioxidant, antimicrobial

1. Introduction

Ferrites, a ferrimagnetic ceramic with the general formula MFe_2O_4 (M stands for bivalent metal ions such as Mn, Fe, Co, Ni, Cu, and Zn), are widely known for their physical and magnetic properties, electrical resistivity, and great chemical stability. Ferrites have garnet, hexagonal, and spinel structures based on their original crystal lattice. Among these structures, normal and inverse spinel ferrites are particularly attractive [1,2]. Spinel ferrite nanoparticles (SFNPs) are metal oxides with a spinel structure and general formula AB_2O_4, where A and B represent different metal cations located tetrahedral (A-site) and octahedral (B-site) respectively, containing at least iron chemical formula. Metal cations are coupled to oxygen atoms at both sites tetrahedrally and octahedrally. The physicochemical features of ferrites are largely reliant on the metal cation types, quantities, and positions in the crystalline structure. [3]. Magnetic transition oxide nanostructures with spinel structure MFe_2O_4 (M = Zn, Mn, Ni, Co, etc.) possess unique magnetic properties such as high coercivity, single domain effects, moderate magnetization, spin filtering, superparamagnetism, etc., resulting in impressive results for industrial and biological applications [4].

The structures of the spinels usually consist of two types: normal and inverse. The ions M^{2+} and Fe^{3+} are inserted at the A and B sites of the normal spinel. M^{2+} cations and Fe^{3+} cations are located at A and B sites in normal spinel. In inverse spinel, M^{2+} cations are located in the B area and Fe^{3+} cations at both A and B sites depending upon the preparation method [5,6]. The spinel ferrites are described by the formula $(A)[B]_2O_4$, where (A) and [B] indicate cations in tetrahedral and octahedral sites, respectively, of cubic oxygen close packing. Bulk $ZnFe_2O_4$ has a normal spinel structure with all Zn^{2+} ions in the A-sites and Fe^{3+} ions in the B-sites. However, unlike the bulk material, the nanocrystalline $ZnFe_2O_4$ always has a partially inverse spinel structure in which Zn^{2+} and Fe^{3+} ions are distributed over the A and B sites, with the following formula: $(Zn^{2+}_{1-\delta}Fe^{3+}_{\delta})[Zn^{2+}_{\delta}Fe^{3+}_{2-\delta}]O_2^{-4}$ where δ is the inversion coefficient defined as the fraction of (A) sites occupied by Fe^{3+} cations and depends on crystallite size and method Preparation

Received: August 10, 2023
Received in revised: September 08, 2023
Accepted: September 09, 2023

[7]. The spinal ferrites were prepared bysol–gel processing [7] polymer matrix precipitation [8], coprecipitation [9], solid-state reaction [10], a wet-milling method [6], hydrothermal crystallization [11], citrate composition [12]. Due to its special properties such as chemical and thermal stability and the dependence of the magnetic properties on the particle size, spinel ferrite has considerable potential for a variety of technical applications, such as magnetic resonance imaging (MRI), photo-induced transformers, and ferrofluids [13]. Widespread bioapplications such as magnetically controlled drug delivery, high-density magnetic recording media, hyperthermia, and have generated increased interest in these materials due to their unique structure and magnetic capabilities [14].

An important class of heterocyclic chemicals, xanthenes, and its derivatives are used in biological applications like anti-inflammatory [15], antibacterial activities [16], antifungal and antibacterial activity [17], antidiabetic activity [18], antioxidant activity [19], antiviral activity [20], antiparasitic activity [21], and antihistaminic activity [22].

Until now, several researchers have described various techniques for preparing various xanthene derivatives. For example, under ultrasound irradiation, ceric ammonium nitrate as a catalyst [23], under solvent-free conditions and $ZrOCl_2 \cdot 8H_2O$ as a catalyst [24], catalyzed by diammonium hydrogen phosphate [25], under microwave irradiation [26], catalyzed by ZrO_2/SO_4^{2-}/Co nanoparticles [27] catalyzed by Bronsted Acidic Ionic Liquids (BAILs) [28], using cobalt (II) complex containing an ionic liquid [29], polymeric catalyst [30], and under solvent-free conditions in the presence of trichloromelamine (TCM) [31].

Designing safe and inexpensive methods for synthesizing xanthenes using environmentally friendly and efficient catalysts has become of crucial importance in recent years. spinel ferrites are very useful as a catalyst in the synthesis of organic compounds because of their high efficiency, especially their super magnetic properties, fast separation, and recyclability. In this context, we prepared a $ZnFe_2O_4$@Fe_3O_4 as a heterogeneous catalyst for the synthesis of 1,8-dioxo-octahydroxanthenes analogs and investigated the biological activity of 1,8-dioxo-octahydroxanthenes including antibacterial and antioxidant activity.

2. Experimental

2.1. Materials

The Iron dichloride tetrahydrate ($FeCl_2 \cdot 4H_2O$), zinc chloride ($ZnCl_2$), iron chloride hexahydrate ($FeCl_3 \cdot 6H_2O$), and sodium hydroxide (NaOH) were provided by Merck Company. Dimedone, all solvents, and other reagents were provided by Merck and Sigma-Aldrich Company.

2.2. Preparations of zinc ferrite ($ZnFe_2O_4$)

3.3637 g $FeCl_3.6H_2O$ and 0.8481 g $ZnCl_2$ were dissolved in 50 mL distilled water. The flask was kept under stirring and reflux at 80 °C, the pH of the reaction mixture was raised to about 10 by the addition of 10% NaOH solution, and stirring was continued for 3 h. The precipitate was collected and centrifuged, then washed several times with distilled water and ethanol, and finally dried under vacuum at 100°C for 6 h. The obtained dark brown powders were crushed and then calcined at 450 °C for 3 h (**Figure 1**).

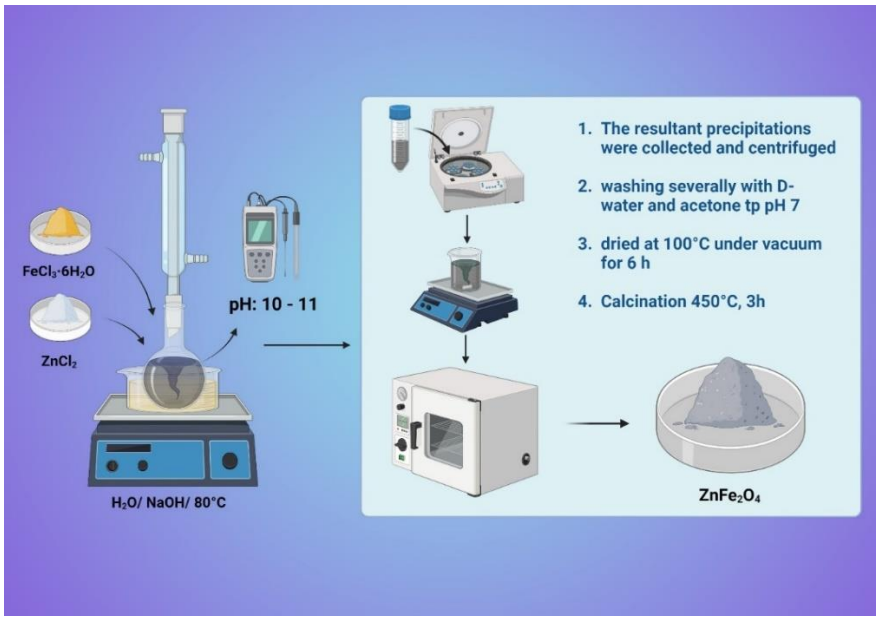

Figure 1. The synthesis procedure of $ZnFe_2O_4$ nanoparticles

2.3. Preparations of Fe_3O_4 magnetic nanoparticles

$FeCl_2.4H_2O$ (1.98 g) and $FeCl_3.6H_2O$ (5.4 g) in a 1:2 molar ratio were dissolved in 50 mL deionized water, the mixture was mechanically stirred at 80° C for 15 min and NaOH solution (1M) was added to the mixture until the pH reached 10. After 30 min, the black precipitate was separated by magnetic decantation washed several times with deionized water and ethanol, and dried under a vacuum at 80 °C for 10 h.

2.4. Preparations of $ZnFe_2O_4$@Fe_3O_4

For the synthesis of $ZnFe_2O_4$@Fe_3O_4 with a 2:1 weight ratio of $ZnFe_2O_4$ and Fe_3O_4, 0.23 g of magnetite nanoparticles (Fe_3O_4) and 0.47 g of zinc ferrite nanoparticles ($ZnFe_2O_4$) were added to 20 mL of deionized water. The reaction mixture was dispersed for 1 h. Then the pH of the reaction mixture was adjusted to 8 with NaOH solution (1M) and stirred under reflux conditions for 3 h. Finally, $ZnFe_2O_4$@Fe_3O_4 nanoparticles were collected from the reaction vessel using an external magnet then washed several times with distilled water and dried in an oven at 80 °C (**Figure 2**).

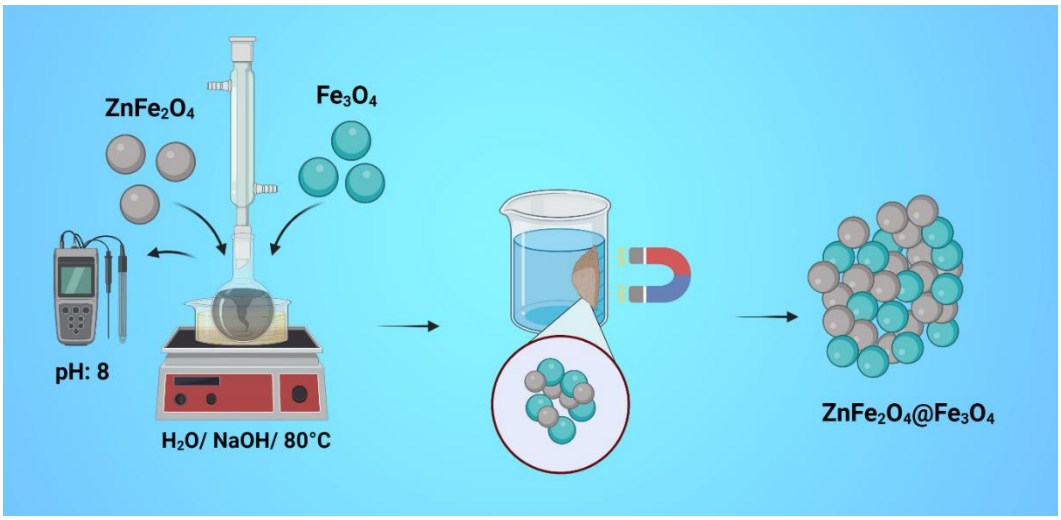

Figure 2. The synthesis procedure of $ZnFe_2O_4$@Fe_3O_4 nanoparticles

2.5. General procedure for the synthesis of 1,8-dioxo-octahydroxanthene derivatives

Dimedone or 1,3 cyclohexanedione (2 mmol), an aldehyde (1 mmol), and $ZnFe_2O_4@Fe_3O_4$ (0.06 g) in EtOH (5 mL) were combined. The reaction mixture was stirred at reflux conditions and checked for completion by thin-layer chromatography (hexane/ethyl acetate 5:1). After the completion of the reaction, the catalyst was separated with an external magnet. The crude solid product was filtered and then purified by recrystallization from ethanol (**Scheme 1**).

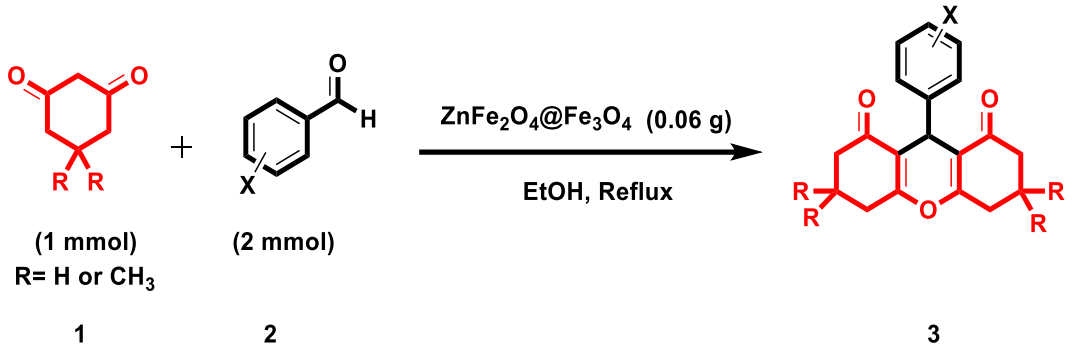

Scheme 1. Synthesis of 1,8-dioxo-octahydroxanthenes

3. Results and discussion

3.1. Description of catalysts

FTIR: FT-IR spectra of prepared zinc ferrite and $ZnFe_2O_4@Fe_3O_4$ are revealed in **Figure 3A**. The broad bands around 3450 and 3429 cm^{-1} in the spectrum of $ZnFe_2O_4$ and $ZnFe_2O_4@Fe_3O_4$ respectively, are related to stretching vibrations of the hydroxyl group. The absorption peaks at 1633 cm^{-1} in $ZnFe_2O_4$ and 1607 cm^{-1} in $ZnFe_2O_4@Fe_3O_4$ correspond to the hydroxyl group's bending vibrations [32]. Metal oxide vibrations typically occur below 1000 cm^{-1}. Fe-O-H bending vibrations occur at 797 cm^{-1} [33]. The weak signal at 556 cm-1 is identified as a Fe-O vibration [34].

XRD: **Figure 3B** shows the XRD patterns of the $ZnFe_2O_4$ and $ZnFe_2O_4@Fe_3O_4$. The peaks observed at 2θ range of 18.55 º, 30.32 º, 35.51 º, 43.18 º, 53.43 º, 56.86 º, 62.51 º, 70.85 º and 73.83 º which related to the plane of reflection (220), (311), (222), (400), (511), (440), (620) and (532), respectively [35]. Fe_3O_4 Nps showed a semi-crystalline nature, in the X-ray diffraction pattern of $ZnFe_2O_4@Fe_3O_4$, the peaks were detected at 2θ of 30.05 º, 35.44 º, 57.37 º, and 62.48 º which corresponds to the plane of reflection (2 2 0), (3 1 1), (5 1 1), and (4 4 0), respectively [36].

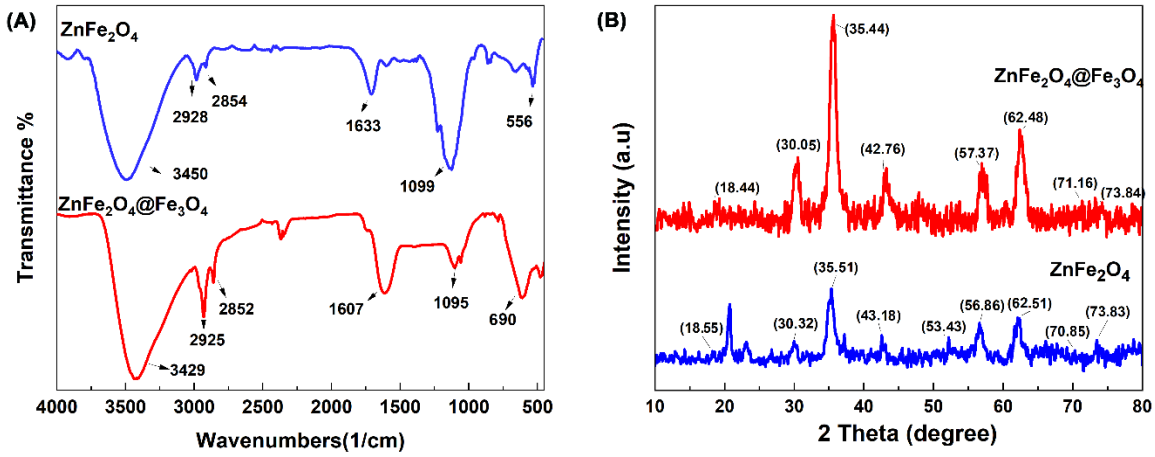

Figure 3. FTIR spectra (**A**) and XRD patterns (**B**) of $ZnFe_2O_4$ and $ZnFe_2O_4@Fe_3O_4$

SEM: Figure 4 shows FESEM images of $ZnFe_2O_4$ and $ZnFe_2O_4@Fe_3O_4$ at two magnifications of 200 nm and 1 μm. FESEM images show almost spherical morphology for both samples. The accumulation of $ZnFe_2O_4$ and $ZnFe_2O_4@Fe_3O_4$ were determined around 20 - 60 nm and 20 -50 nm, respectively.

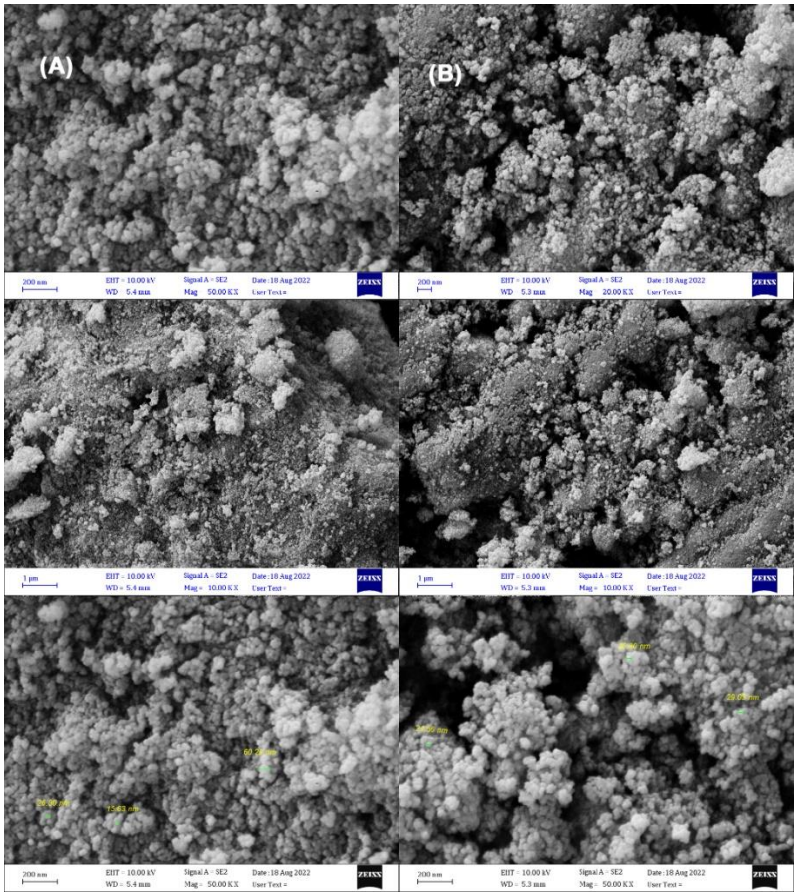

Figure 4. FESEM micrographs of (**A**) $ZnFe_2O_4$ and (**B**) $ZnFe_2O_4@Fe_3O_4$ nanoparticles.

VSM: The VSM curves of Fe_3O_4, $ZnFe_2O_4$, and $ZnFe_2O_4@Fe_3O_4$ are shown in **Figure 5A**. $ZnFe_2O_4$ with a magnetic saturation value of 16.51 emu/g showed less magnetic properties compared to curve $ZnFe_2O_4@Fe_3O_4$ with a magnetic saturation value of 57.17. The VSM curves of $ZnFe_2O_4@Fe_3O_4$ and Fe_3O_4 have a magnetization saturation value of 59.94 emu/g and 57.17, respectively, showing similar magnetic properties.

TGA*:* The TGA curves for $ZnFe_2O_4$ and $ZnFe_2O_4@Fe_3O_4$ are shown in **Figure 5B.** Both curves showed a weight loss of less than 10%. Weight loss at temperatures below 200 °C occurred due to the evaporation of moisture trapped on the surface of the samples.

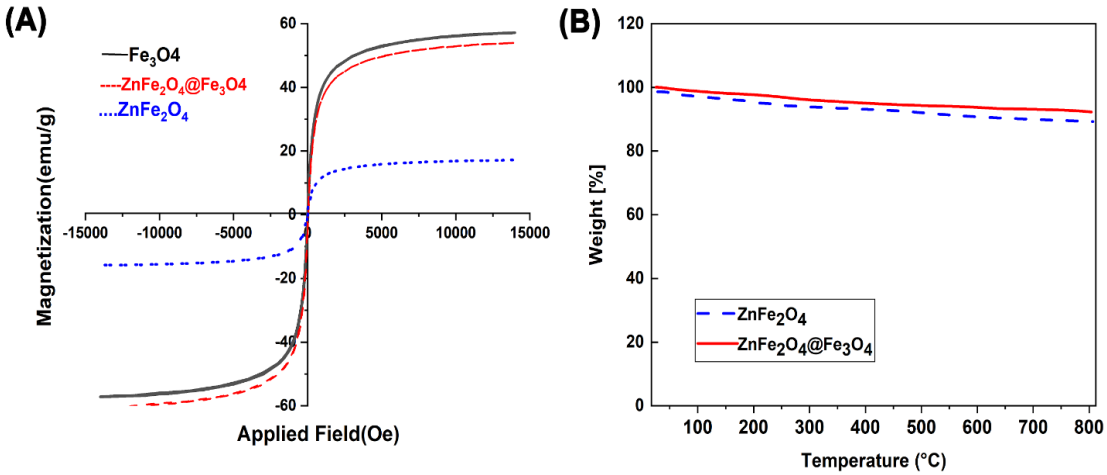

Figure 5. VSM curves of $ZnFe_2O_4$, $ZnFe_2O_4@Fe_3O_4$, and Fe_3O_4 **(A)**, TGA thermograms of $ZnFe_2O_4$ and $ZnFe_2O_4@Fe_3O_4$ **(B)**.

EDX: EDX analysis (**Figure 6**) shows the chemical composition of $ZnFe_2O_4$ and $ZnFe_2O_4@Fe_3O_4$ produced. The existence of different quantities of O, Zn, and Fe elements in the spectra of $ZnFe_2O_4$ and $ZnFe_2O_4@Fe_3O_4$ as well as the increase of Fe in the spectrum of $ZnFe_2O_4@Fe_3O_4$ compared to $ZnFe_2O_4$ has been demonstrated in the spectrum and the tabulated data.

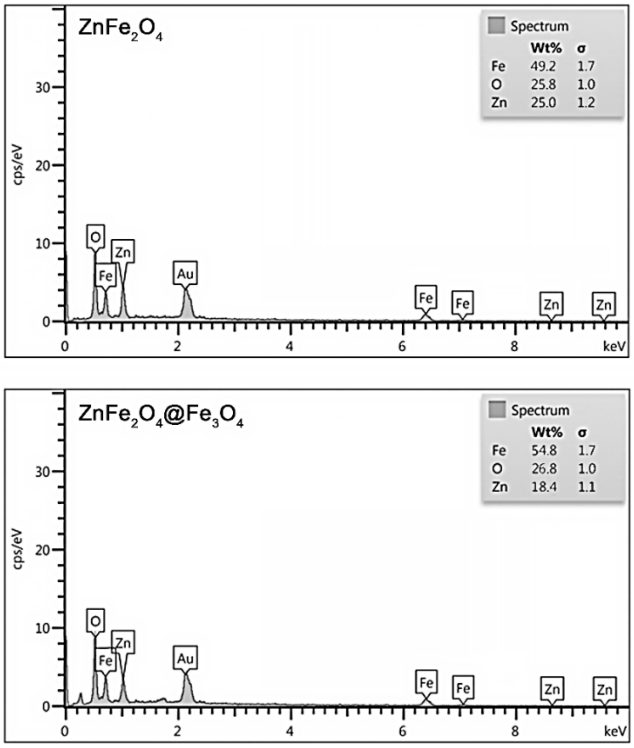

Figure 6. EDX spectra, and tabulated data of $ZnFe_2O_4$ and $ZnFe_2O_4@Fe_3O_4$

3.2. Catalytic potential study of the $ZnFe_2O_4@Fe_3O_4$

After fabrication and characterization, the catalytic efficiency of $ZnFe_2O_4@Fe_3O_4$ in the preparation of 1,8-dioxo-octahydroxanthenes was evaluated. A one-pot multicomponent organic process with dimedone (2 mmol), and benzaldehyde (1 mmol) was used as a model reaction to optimize various conditions (**Table 1**). To recognize and

observe the catalytic effect of $ZnFe_2O_4$@Fe_3O_4 in the synthesis of 1,8-dioxo octahydroxanthenes and to determine the optimal catalyst amount on the progress, different amounts of $ZnFe_2O_4$@Fe_3O_4 catalyst in ethanol solvent were used. The results showed that 0.06 g of $ZnFe_2O_4$@Fe_3O_4 was the optimal value for the synthesis of 1,8-dioxo-octahydroxanthenes. The reaction was studied in the presence of different solvents such as EtOH, H_2O, CH_2Cl_2, Hexane, THF, H_2O/EtOH, and without solvents. As shown in **Table 1**, the reaction with EtOH was very effective. This reaction was also tested at 25, 50, and 80 °C temperatures. The highest yield with the shortest reaction time was achieved at 80 °C and a catalyst of 0.06 g in EtOH. The catalytic effect of $ZnFe_2O_4$, and Fe_3O_4 was examined using the synthesis of **3a** (**Entries 14, 15**), and the results showed that in the presence of $ZnFe_2O_4$ were obtained products with the highest efficiency and the shortest time. Considering that one of the purposes of this research is to prepare and produce a catalyst that can be easily separated from the reaction vessel and recovered. Therefore, the priority is to develop a catalyst with its magnetic properties.

Table 1. Optimization of the three-component reaction of dimedone (2 mmol) and benzaldehyde (1 mmol) [a].

Entry	Solvent	Catalyst (g)	Temp /°C	Time (Min)	Yield %[b]
1	EtOH	-	reflux	60	25
2	EtOH	0/02	reflux	60	30
3	EtOH	0/04	reflux	60	65
4	EtOH	0/06	reflux	**30**	**91**
5	EtOH	0/08	reflux	30	92
6	H_2O	0/06	reflux	120	60
7	CH_2Cl_2	0/06	reflux	120	25
8	Hexane	0/06	reflux	120	10
9	THF	0/06	reflux	120	30
10	H_2O/EtOH	0/06	reflux	120	60
11	Solvent-free	0/06	100	120	40
12	EtOH	0/06	25	240	50
13	EtOH	0/06	50	60	70
14	EtOH	($ZnFe_2O_4$) 0/06	reflux	25	92
15	EtOH	(Fe_3O_4) 0/06	reflux	45	80

[a] Reaction conditions: dimedone (2 mmol) and benzaldehyde (1 mmol). [b] isolated yield.

Different aromatic aldehydes were investigated for the synthesis of 1,8-dioxo octahydroxanthenes using the optimal amount of (0.06 g $ZnFe_2O_4$@Fe_3O_4 (**Table 2**). The results showed that the reaction was performed with benzaldehyde derivatives having both electron-donating groups and electron-withdrawing. The products obtained were purified by crystallization in ethanol and identified using spectroscopic techniques (^{1}H NMR and ^{13}C NMR).

Table 2. Synthesis of 1,8-dioxo-octahydroxanthenes by $ZnFe_2O_4$@Fe_3O_4 and aldehyde derivatives [a].

Entry	Product	Code	Time (min.)	Yield[b] (%)	M.P. (°C)		Ref.
					Observed	Reported	
1	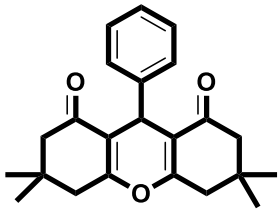	**3a**	30	91	202-204	205-205	[37]

2	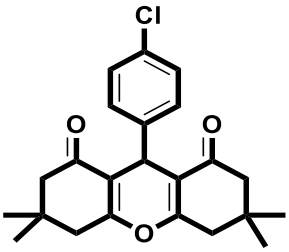	**3b**	20	90	235-236	238-240	[37]
3	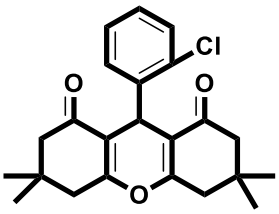	**3c**	25	92	225-228	226-228	[37]
4	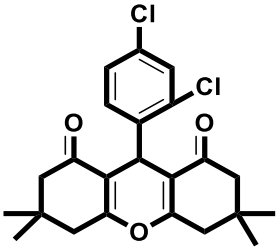	**3d**	20	90	257-259	251-252	[37]
5	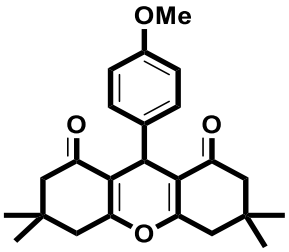	**3e**	30	90	215-216	210-211	[37]
6	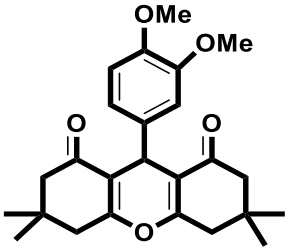	**3f**	35	89	174-176	181-183	[38]
7	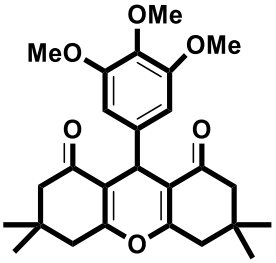	**3g**	40	90	262-264	205-208	[24]
8	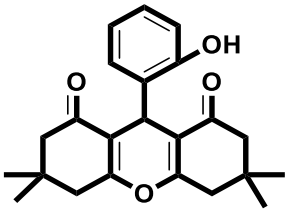	**3h**	45	86	233-235	231-233	[39]

9	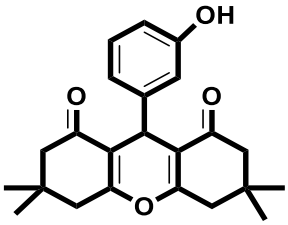	**3i**	40	90	118-120	222-224	[38]
10	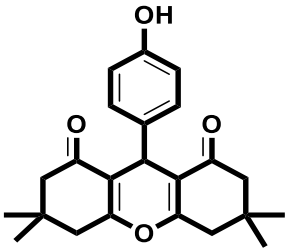	**3j**	45	90	136-138	247-250	[38]
11	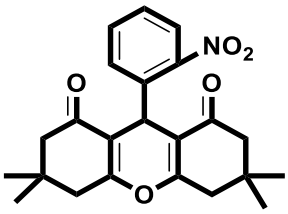	**3k**	15	90	200-202	203-205	[37]
12	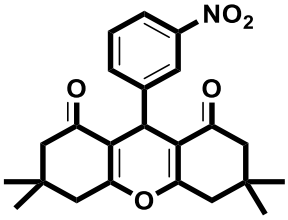	**3l**	15	94	175-176	170-172	[37]
13	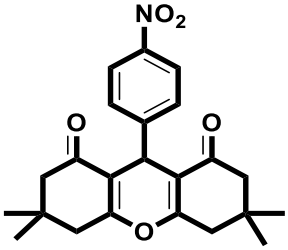	**3m**	15	95	224-226	226-228	[37]
14	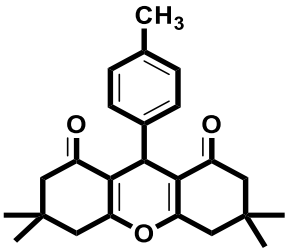	**3n**	45	87	214-216	210-211	[37]
15	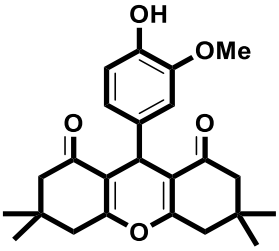	**3o**	40	90	234-236	226-228	[40]

16	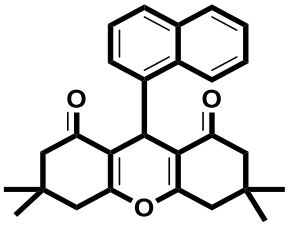	**3p**	60	87	238-240	237-238	[37]
17	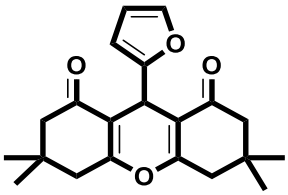	**3q**	30	90	178-180		
18	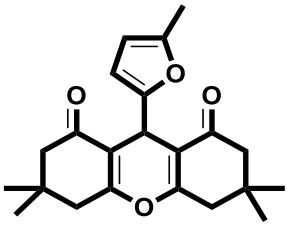	**3r**	35	90	198-200		
19	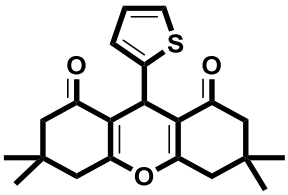	**3s**	40	91	167-169	164-165	[24]
20	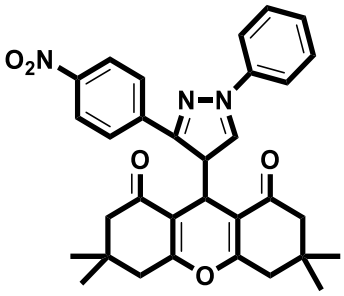	**3t**	60	90	154-156	NR	
21	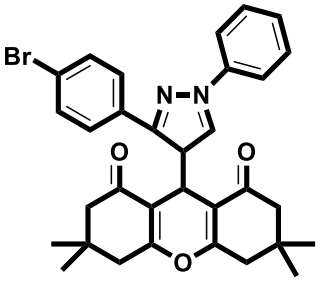	**3u**	60	92	120-122	NR	
22	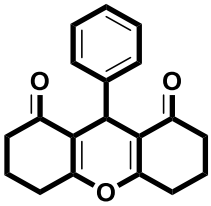	**3v**	35	92	269-272	268-270	[41]

23	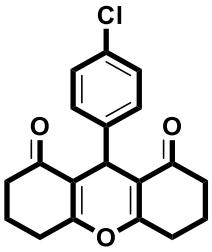	**3w**	25	94	285-287	288-290	[41]
24	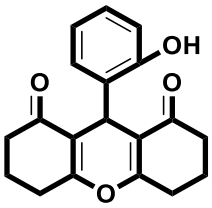	**3x**	50	85	222-223	224-226	[41]
25	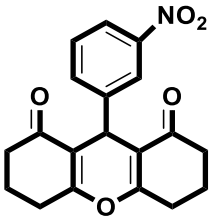	**3y**	35	90	283-285	282-283	[41]

[a] Reaction conditions: dimedone or 1,3 cyclohexanedione (2 mmol), aldehyde (1 mmol), EtOH (5 mL), and catalyst (0.06 g) at 80 °C; [b] isolated yield, NR: not reported.

The use of aromatic aldehydes with electron-withdrawing groups (-4-NO_2 and -3-NO_2) leads to the formation of a product with very high efficiency. In addition, the products have been synthesized in due course using heterocyclic aldehyde compounds such as thiophenecarbaldehyde, furfural, 5-methyl furfural, and pyrazole-4-carbaldehyde. The results showed that aldehydes with electron-withdrawing groups have better efficiency than electron-donating groups. Electron withdrawing groups shorten the reaction time and increase the efficiency of this reaction.

According to the Lewis acidic nature of $ZnFe_2O_4$@Fe_3O_4, a possible mechanism has been suggested (**Figure 7**). It is expected that the reaction of dimedone in enol form with aromatic aldehyde under the influence of $ZnFe_2O_4$@Fe_3O_4 produces ortho-quinone methides **(I)** through the formation of Knoevenagel adduct. Intermediate **I** can further undergo Michael addition with another dimedone molecule to form intermediate **II**. In the end, intermediate **II** was converted into the product by cyclization.

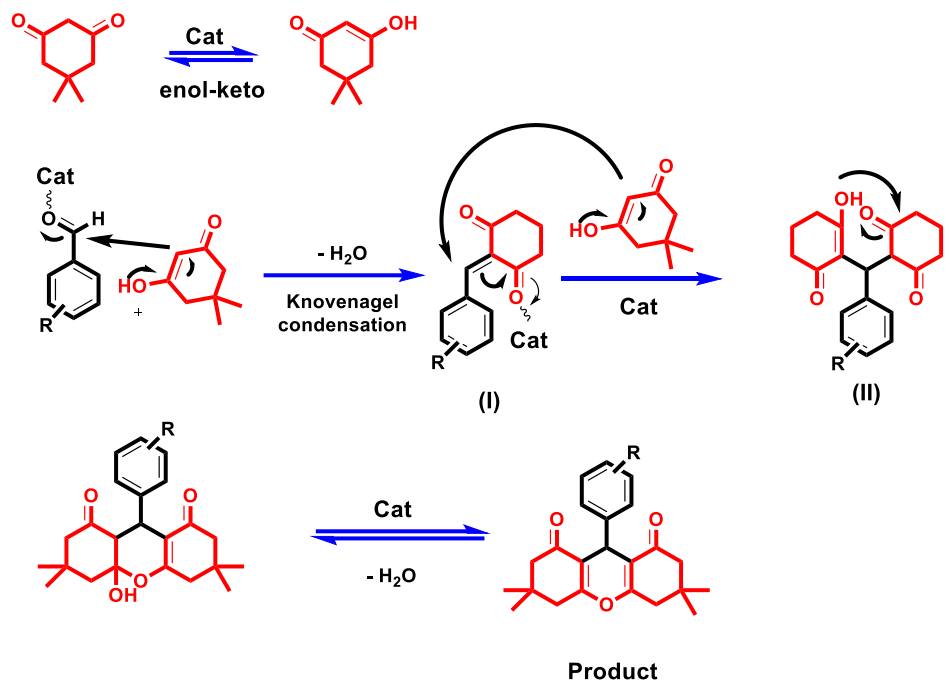

Figure 7. The proposed mechanism for the synthesis of 1,8-dioxo-octahydroxanthene catalyzed by $ZnFe_2O_4@Fe_3O_4$.

Comparison of the catalytic efficiency of $ZnFe_2O_4@Fe_3O_4$ with various catalysts reported for the synthesis of 1,8-dioxo-octahydroxanthenes

To show the efficiency of this method in comparison with reported methods, we used the reaction of dimedone(2 mmol) and benzaldehyde (1 mmol) for the synthesis of **3a** as a model. This comparison is shown in **Table 3**. It is clear from the data that our method has shorter reaction times and provides higher yields of the products.

Table 3. Comparison of the catalytic efficiency of $ZnFe_2O_4@Fe_3O_4$ with various catalysts reported for the synthesis of 3a.

Entry	Catalyst	Condition	Yield %	Time Min.	Ref.
1	$ZnFe_2O_4@Fe_3O_4$ (0.06 g)	EtOH/ 80 °C	91	30	This study
2	Sawdust sulphonic acid	EtOH/ 80 °C	88	50	[42]
3	$SmCl_3$	Neat/ 120 °C	98	540	[43]
4	Ionic liquid [TMXH][TSA	Solvent-free at 110 °C	87	20	[44]
5	SO_4^{2-}/ZrO_2	EtOH/ 80 °C	95	450	[45]
6	Tetrabutylammonium hydrogen sulfate	Water/ reflux	88	210	[46]

Recovery: From an economic point of view, the reusability of heterogeneous catalysts is of great importance. In this context, the reusability and recycling of $ZnFe_2O_4@Fe_3O_4$ for the synthesis of derivative **3a** was investigated. After the reaction, $ZnFe_2O_4@Fe_3O_4$ was separated from the reaction vessel by a magnet and used after washing with EtOH for 5 consecutive cycles (**Figure 8**). The results indicate that the catalytic potential of the catalyst is very slightly reduced.

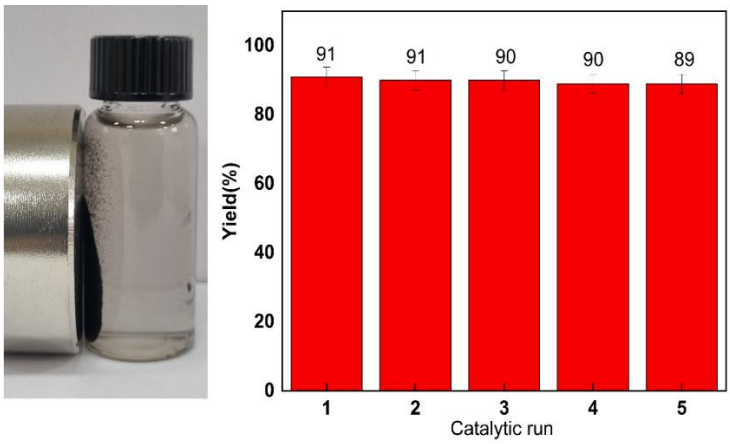

Figure 8. $ZnFe_2O_4@Fe_3O_4$ reusability in the synthesis of 3a

To prove the stability of the catalyst after recovery, the FTIR spectrum and XRD pattern of the $ZnFe_2O_4@Fe_3O_4$ catalyst were recorded (**Figure 9**). As seen in the FTIR spectrum and XRD pattern, very few differences in the nanocatalyst characteristic peaks signify the stability of the catalyst.

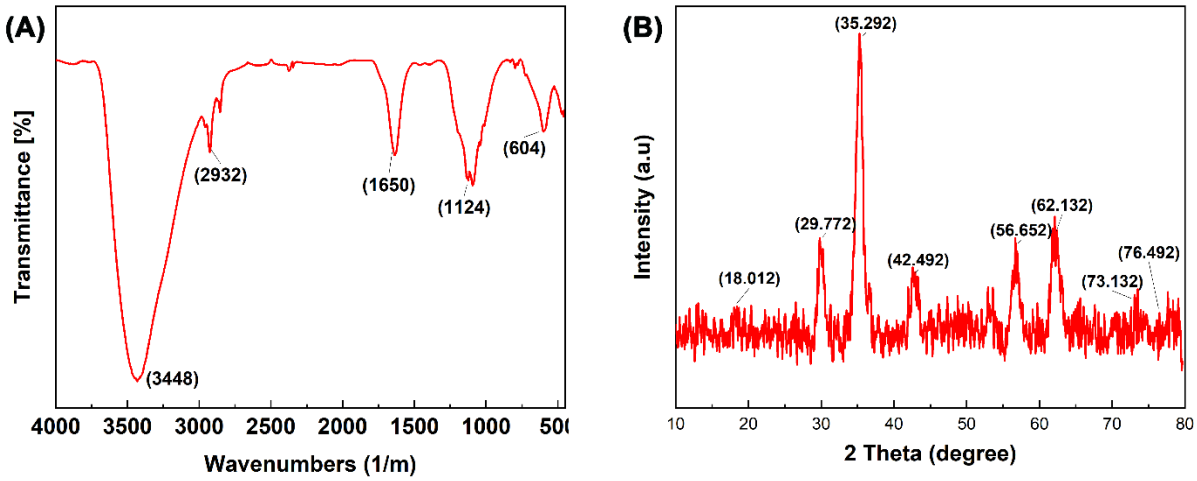

Figure 9. The FTIR spectrum (**A**) and XRD pattern (**B**) of the $ZnFe_2O_4@Fe_3O_4$ after recovery.

3.3. Antioxidant activity

The potential of organic compounds for use in pharmaceutical substances can be increased through antioxidant abilities [47]. As a result, the antioxidant activity of the 1,8-dioxo-octahydroxanthenes in the DPPH ethanolic solution was examined (**Figure 10**). The results indicated that between 64.4% and 90.2% of the compounds had antioxidant properties.

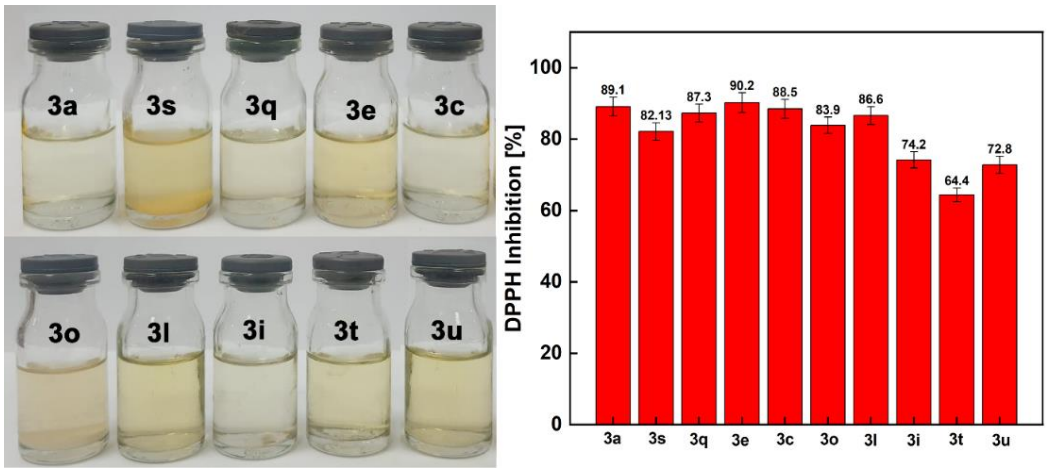

Figure 10. Antioxidant activities of prepared 1,8-dioxo-octahydroxanthenes.

3.4. Antibacterial activity

Table 4 and **Figure 11** display the findings of the disk diffusion method's evaluation of the 1,8-dioxo-octahydroxanthene derivatives' antibacterial activity against *E. faecalis*, *E. coli*, *L. monocytogenes*, *S. enterica*, and *S. aureus*. The 1,8-dioxo-octahydroxanthenes have no antibacterial activity on *E. faecalis* and *E. coli*, while **3c** and **3l** have inhibitory effects on the growth of *L. monocytogenes*, *S. aureus*, and *S. enterica*.

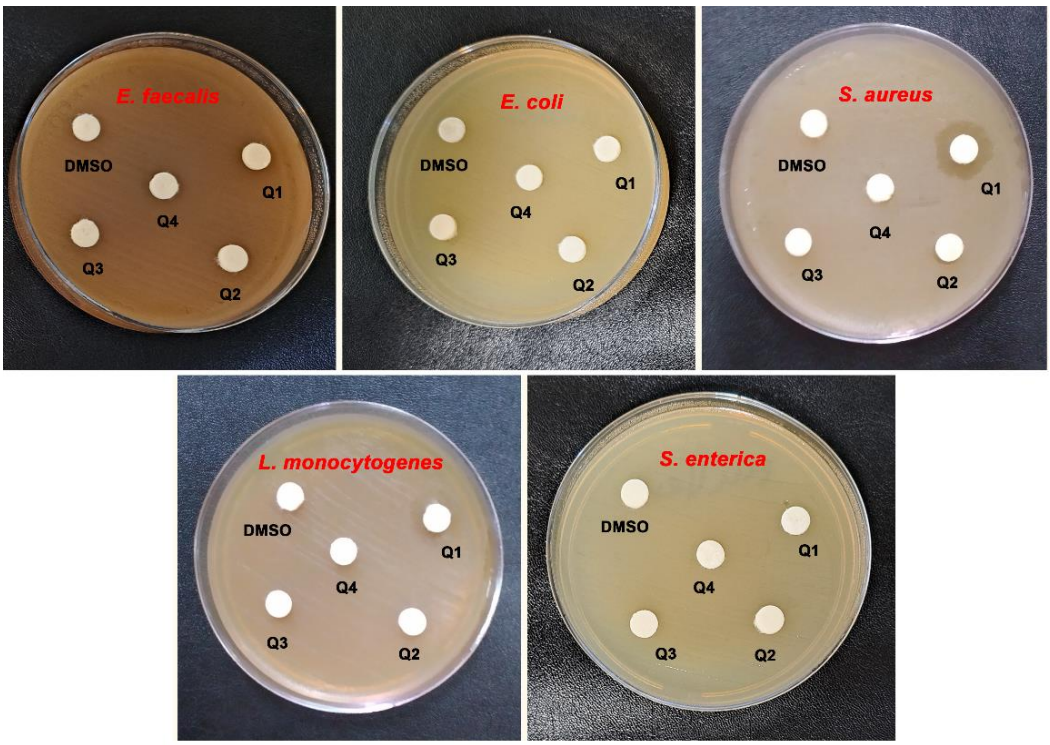

Figure 11. Kirby-Bauer disk diffusion test of 1,8-dioxo-octahydroxanthene's.

Table 4. Antibacterial activity data of 1,8-dioxo-octahydroxanthenes.

Derivatives	*E. coli*	*S. enterica*	*L. monocytogenes*	*S. aureus*	*E. faecalis*
	Diameter of growth inhibition of zone (mm)				
3c	NE	NE	2±0.2	3±0.1	NE
3g	NE	NE	NE	NE	NE
3o	NE	NE	NE	NE	NE
3l	NE	NE	14±1.1	13±1.2	NE
Antibiotic discs (Positive controls)					
TMP5	17±0	27±0.0	40±0.0	17±0.0	34±0.0
GM10	25±0	25±0.0	34±0.0	21±0.0	22±0.0
SXT	25±0	44±0.0	44±0.0	28±0.0	36±0.0
Solvent (Negative control)					
DMSO	NE	NE	NE	NE	NE

NE: No effect

4. Conclusion

A magnetic catalyst for the synthesis of 1,8-dioxo-octahydroxanthenes was prepared from the composite of the spinel-ferrite nanoparticles $ZnFe_2O_4$ with Fe_3O_4 nanoparticles. According to the VSM results, the catalyst exhibits good magnetic properties. The TGA curves for $ZnFe_2O_4$@Fe_3O_4 also indicated high thermal stability. Evidence shows that smaller nanoparticles strongly tend to aggregate/agglomerate at different grain sizes. Therefore, the possibility of aggregation/agglomeration in smaller nanoparticles is much higher compared to larger particles, and this is considered a limitation in the use of $ZnFe_2O_4$@Fe_3O_4 nanocatalyst. Given the good catalytic properties of the nanocatalyst $ZnFe_2O_4$@Fe_3O_4 as a Lewis acid in the synthesis of organic compounds and its excellent magnetic properties, various catalysts can be designed by functionalizing the prepared composite. The 1,8-dioxo-octahydroxanthenes were produced by one-pot condensation in the existence of 0.06 g $ZnFe_2O_4$@Fe_3O_4, the desired products were prepared under optimal reaction conditions in a short time (15-60 min), also new 1,8-dioxo–octahydroxanthenes were attained in good yields (90–92 %) using pyrazole-4-carbaldehydes. The 1,8-dioxo-octahydroxanthenes illustrated antioxidant activity ranging from 64.4% to 90.2%. In addition, some 1,8-dioxo-octahydroxanthenes were active against *L. monocytogenes, S. aureus, and S. enterica*.

Spectroscopic Data

3a, Figure S1, S2: Solid, m.p. 202-204 °C; ^{1}H NMR (400 MHz, DMSO-d_6): δ (ppm) 0.89 (s, 6H, CH_3), 1.03 (s, 6H, CH_3), 2.05-2.10 (d, 2H, J=16 Hz, CH_2), 2.24-2.26 (d, 2H, J=16 Hz, CH_2), 2.49-2.60 (m, 4H, CH_2), 4.52 (s, 1H, benzylic), 7.08-7.11 (m, 1H, aromatic), 7.16-7.23 (m, 4H, aromatic). ^{13}C NMR (100 MHz, DMSO-d_6): 26.98,28.25, 29.14, 47.00, 50.47, 114.87, 126.65, 126.87, 128.33, 128.51, 144.72, 163.38, 187.74, 196.54.

3b, Figure S3: Solid, m.p.235-236 °C; ^{1}H NMR (400 MHz, DMSO-d_6): δ (ppm) 0.83 (s, 6H, CH_3), 1.00 (s, 6H, CH_3), 1.95-1.99 (d, 2H, J=16 Hz, CH_2), 2.15-2.19 (d, 2H, J=16 Hz, CH_2), 2.26-2.30 (d, 2H, J=16 Hz, CH_2), 2.40-2.50 (m, 2H, CH_2), 4.84 (s, 1H, benzylic), 7.15-7.17 (d, 2H, J=8 Hz, aromatic), 7.23-7.25 (d, 2H, J=8 Hz, aromatic).

3m, Figure S4, S5: Solid, m.p. 224-226 °C; ^{1}H NMR (400 MHz, DMSO-d_6): δ (ppm) 0.90 (s, 6H, CH_3), 1.04 (s, 6H, CH_3), 2.06-2.10 (d, 2H, J=16 Hz, CH_2), 2.26-2.30 (d, 2H, J=16 Hz, CH_2), 2.50-2.63 (m, 4H, CH_2), 4.62 (s, 1H, benzylic), 7.45-7.47 (d, 2H, J=8 Hz, aromatic), 8.10-8.12 (d, 2H, J=8 Hz, aromatic). ^{13}C NMR (100 MHz, DMSO-d_6): 27.01, 29.03, 32.37, 50.33, 113.80, 123.63, 129.97, 146.41, 152.26, 163.93, 196.57.

3o, Figure S6, S7: Solid, m.p. 234-236 °C; ^{1}H NMR (400 MHz, DMSO-d_6): δ (ppm) 1.01 (s, 6H, CH_3), 1.04 (s, 6H, CH_3), 2.05-2.10 (d, 2H, J=16 Hz, CH_2), 2.24-2.26 (d, 2H, J=16 Hz, CH_2), 2.28-2.32 (d, 2H, J=16 Hz, CH_2), 2.42-2.50 (m, 2H, CH_2), 3.65(s, 3H, OMe), 4.72 (s, 1H, benzylic), 6.50-6.55 (m, 2H, aromatic), 6.70 (m, 1H, aromatic), 8.59 (s, 1H, OH). ^{13}C NMR (100 MHz, DMSO-d_6): 26.82, 29.22, 29.66, 32.38, 32.58, 50.78, 55.94, 56.51, 112.25, 112.66, 115.22, 120.24, 1.8.98, 144.80, 147.16, 149.47, 194.96, 196.62 ppm.

3p, Figure S8*:* Solid, m.p.238-240 °C; ^{1}H NMR (400 MHz, DMSO-d_6): δ (ppm) 0.8 (s, 6H, CH_3), 1.03 (s, 6H, CH_3), 1.96-2.00 (d, 2H, J=16 Hz, CH_2), 2.21-2.26 (d, 2H, J=16.4 Hz, CH_2), 2.50-2.52 (d, 2H, J=6.8 Hz, CH_2), 2.56-2.66 (m, 2H, CH_2), 5.32 (s, 1H, benzylic), 7.16-7.18 (d, 1H, J=7.2 Hz, aromatic), 7.37-7.41 (t, 1H, J=8 Hz, aromatic), 7.47-

7.51 (t, 1H, *J*=8 Hz, aromatic), 7.57-7.60 (t, 1H, *J*=8 Hz, aromatic), 7.68-7.70 (d, 1H, *J*=8 Hz, aromatic), 7.82-7.84 (d, 1H, *J*=8 Hz, aromatic), 8.67-8.69 (d, 1H, *J*=8 Hz, aromatic).

3t, Figure S9, S10*:* Solid, m.p.154-156 °C; ^{1}H NMR (400 MHz, DMSO-d_6): δ (ppm) 0.95 (s, 6H, CH_3), 1.07 (s, 6H, CH_3), 2.07-2.11 (d, 2H, *J*=16 Hz, CH_2), 2.19-2.23 (d, 2H, *J*=16.4 Hz, CH_2), 2.50-2.52 (d, 4H, *J*=6.8 Hz, CH_2), 4.67 (s, 1H, benzylic), 7.30 (t, 1H, *J*=8 Hz, aromatic), 7.48 (t, 2H, *J*=8 Hz, aromatic), 7.82-7.84 (d, 2H, *J*=8 Hz, aromatic), 8.35-8.43 (m, 5H, aromatic). ^{13}C NMR (100 MHz, DMSO-d_6): 19.02, 22.36, 27.50, 28.78, 32.37, 50.53, 56.50, 114.90, 118.57, 123.81, 126.87, 128.23, 129.05, 129.87, 129.98, 139.64, 141.72, 147.09, 149.34, 162.79, 197.13 ppm.

3w, Figure S11, S12*:* Solid, m.p.285-287 °C; ^{1}H NMR (400 MHz, DMSO-d_6): δ (ppm) 1.80-1.99 (m, 4H, CH_2), 2.21-2.35 (m, 4H, CH_2), 2.56-2.71 (m, 4H, CH_2), 4.55 (s, 1H, benzylic), 7.19-7.21 (d, 2H, *J*=8 Hz, aromatic), 7.26-7.28 (d, 2H, *J*=8 Hz, aromatic). ^{13}C NMR (100 MHz, DMSO-d_6): 20.30, 26.91, 31.06, 36.82, 115.53, 128.36, 130.40, 131.19, 143.98, 165.48, 196.82 ppm.

3x, Figure S13, S14*:* Solid, m.p. 222-223 °C; ^{1}H NMR (400 MHz, DMSO-d_6): δ (ppm) 1.67-1.73 (m, 2H, CH_2), 1.78-1.97 (m, 2H, CH_2), 2.11-2.41 (m, 6H, CH_2), 2.50-2.57 (m, 2H, CH_2), 5.08 (s, 1H, benzylic), 6.93-6.98 (m, 3H, aromatic, OH), 7.80-7.12(m, 2H, aromatic). ^{13}C NMR (100 MHz, DMSO-d_6): 19.04, 20.75, 20.86, 25.80, 27.72, 37.13, 56.49, 112.43, 115.70, 124.71, 126.20, 127.32, 128.89, 150.04, 167.08, 196.47 ppm.

Authors' contributions

All authors contributed to data analysis, drafting, and revising of the paper and agreed to be responsible for all the aspects of this work.

Declaration of competing interest

The authors declare no competing interest.

Funding

This paper received no external funding.

Data availability

Data will be made available on request.

References

[1] M. Asadi Nasr, M. Deinavizadeh, A.R. Kiasat, Fe3O4@SiO2/DABCO(OH) Core-shell hybrid nanocomposite: Efficient nanomagnetic and basic reusable catalyst in the one-pot synthesis of trithiocarbonate derivatives, Mater. Chem. Horizons, 2(2) (2023) 81-92.

[2] K. Hatami Kahkesh, Z. Baghbantaraghdari, D. Jamaledin, F. Dabbagh Moghaddam, N. Kaneko, M. Ghovvati, Synthesis, characterization, antioxidant and antibacterial activities of zinc ferrite and copper ferrite nanoparticles, Mater. Chem. Horizons, 2(1)(2023) 49-56.

[3] K.K. Kefeni, B.B. Mamba, Photocatalytic application of spinel ferrite nanoparticles and nanocomposites in wastewater treatment: Review, Sustain. Mater. Technol. 23 (2020) e00140.

[4] G. Shahane, K. Zipare, J. Dhumal, S. Bandgar, V. Mathe, G. Shahane, Superparamagnetic Manganese Ferrite Nanoparticles : Synthesis and Magnetic Properties Superparamagnetic Manganese Ferrite Nanoparticles : Synthesis and Magnetic Properties, 4 (n.d.) 2–7.

[5] T.F. Marinca, I. Chicinaş, O. Isnard, Structural and magnetic properties of the copper ferrite obtained by reactive milling and heat treatment, Ceram. Int. 39 (2013) 4179–4186.

[6] M. Mozaffari, H. Masoudi, Zinc Ferrite Nanoparticles: New Preparation Method and Magnetic Properties, J. Supercond. Nov. Magn. 27 (2014) 2563–2567.

[7] M. Atif, S.K. Hasanain, M. Nadeem, Magnetization of sol-gel prepared zinc ferrite nanoparticles: Effects of inversion and particle size, Solid State Commun. 138 (2006) 416–421.

[8] S. Roy, J. Ghose, Mössbauer study of nanocrystalline cubic $CuFe_2O_4$ synthesized by precipitation in polymer matrix, J. Magn. Magn. Mater. 307 (2006) 32–37.

[9] K. Sathiyamurthy, C. Rajeevgandhi, S. Bharanidharan, P. Sugumar, S. Subashchandrabose, Electrochemical and Magnetic Properties of Zinc Ferrite Nanoparticles through Chemical Co-Precipitation Method, Chem. Data Collect. 28 (2020) 100477.

[10] F. Li, H. Wang, L. Wang, J. Wang, Magnetic properties of $ZnFe_2O_4$ nanoparticles produced by a low-temperature solid-state reaction method, J. Magn. Magn. Mater. 309 (2007) 295–299.

[11] A. Phuruangrat, B. Kuntalue, S. Thongtem, T. Thongtem, Synthesis of cubic $CuFe_2O_4$ nanoparticles by microwave-

hydrothermal method and their magnetic properties, Mater. Lett. 167 (2016) 65–68.
[12] D. Thapa, N. Kulkarni, S.N. Mishra, P.L. Paulose, P. Ayyub, Enhanced magnetization in cubic ferrimagnetic $CuFe_2O_4$ nanoparticles synthesized from a citrate precursor: The role of Fe2+, J. Phys. D. Appl. Phys. 43 (2010).
[13] M. Ebrahimi, R. Raeisi Shahraki, S.A. Seyyed Ebrahimi, S.M. Masoudpanah, Magnetic properties of zinc ferrite nanoparticles synthesized by coprecipitation method, J. Supercond. Nov. Magn. 27 (2014) 1587–1592.
[14] M. Amiri, M. Salavati-Niasari, A. Akbari, Magnetic nanocarriers: Evolution of spinel ferrites for medical applications, Adv. Colloid Interface Sci. 265 (2019) 29–44.
[15] A.G. Banerjee, L.P. Kothapalli, P.A. Sharma, A.B. Thomas, R.K. Nanda, S.K. Shrivastava, V. V. Khatanglekar, A facile microwave assisted one pot synthesis of novel xanthene derivatives as potential anti-inflammatory and analgesic agents, Arab. J. Chem. 9 (2016) S480–S489.
[16] S. Naseem, M. Khalid, M.N. Tahir, M.A. Halim, A.A.C. Braga, M.M. Naseer, Z. Shafiq, Synthesis, structural, DFT studies, docking and antibacterial activity of a xanthene based hydrazone ligand, J. Mol. Struct. 1143 (2017) 235–244.
[17] S.N. Richardson, T.K. Nsiama, A.K. Walker, D.R. McMullin, J.D. Miller, Antimicrobial dihydrobenzofurans and xanthenes from a foliar endophyte of Pinus strobus, Phytochemistry. 117 (2015) 436–443.
[18] Y. Kwon, P. Song, J.H. Yoon, J. Ghim, D. Kim, B. Kang, T.G. Lee, J.A. Kim, J.K. Choi, I.K. Youn, H.K. Lee, S.H. Ryu, Xanthene derivatives increase glucose utilization through activation of LKB1-dependent AMP-activated protein kinase, PLoS One. 9 (2014) 1–8.
[19] J.M. Khurana, A. Chaudhary, A. Lumb, B. Nand, Efficient one-pot syntheses of dibenzo[a, i]xanthene-diones and evaluation of their antioxidant activity, Can. J. Chem. 90 (2012) 739–746.
[20] A.A. Carr, J.F. Grunwell, A.D. Sill, D.R. Meyer, F.W. Sweet, B.J. Scheve, J.M. Grisar, R.W. Fleming, G.D. Fleming, Bis-Basic-Substituted Polycyclic Aromatic Compounds. A New Class of Antiviral Agents. 7. Bisalkamine Esters of 9-Oxoxanthene-2,7-dicarboxylic Acid, 3,6-Bis-Basic Ethers of Xanthen-9-one, and 2,7-Bis(aminoacyl)xanthen-9-ones, -xanthenes, and -thioxanthene, J. Med. Chem. 19 (1976) 1142–1148.
[21] K. Chibale, M. Visser, V. Yardley, S.L. Croft, A.H. Fairlamb, Synthesis and evaluation of 9,9-dimethylxanthene tricyclics against trypanothione reductase, Trypanosoma brucei, Trypanosoma cruzi and Leishmania donovani, Bioorganic Med. Chem. Lett. 10 (2000) 1147–1150.
[22] F.J. Villani, T.A. Mann, E.A. Wefer, J. Hannon, L.L. Larca, M.J. Landon, W. Spivak, D. Vashi, S. Tozzi, G. Danko, M. del Prado, R. Lutz, Benzopyranopyridine Derivatives. 1. Aminoalkyl Derivatives of the Azaxanthenes as Bronchodilating Agents, J. Med. Chem. 18 (1975) 1–8.
[23] N. Mulakayala, G. Pavan Kumar, D. Rambabu, M. Aeluri, M. V. Basaveswara Rao, M. Pal, A greener synthesis of 1,8-dioxo-octahydroxanthene derivatives under ultrasound, Tetrahedron Lett. 53 (2012) 6923–6926.
[24] H.Y. Lü, J.J. Li, Z.H. Zhang, $ZrOCl\cdot 28H_2O$: A highly efficient catalyst for the synthesis of 1,8-dioxo-octahydroxanthene derivatives under solvent-free conditions, Appl. Organomet. Chem. 23 (2009) 165–169.
[25] F. Darviche, S. Balalaie, F. Chadegani, P. Salehi, Diammonium Hydrogen Phosphate as a Neutral and Efficient Catalyst for Synthesis of 1,8-Dioxo-octahydroxanthene Derivatives in Aqueous Media, Synth. Commun. 37 (2007) 1059–1066.
[26] A.N. Dadhania, V.K. Patel, D.K. Raval, Ionic liquid promoted facile and green synthesis of 1,8-dioxo-octahydroxanthene derivatives under microwave irradiation, J. Saudi Chem. Soc. 21 (2017) S163–S169.
[27] M.A. Nasseri, M. Kazemnejadi, B. Mahmoudi, F. Assadzadeh, S.A. Alavi, A. Allahresani, Efficient preparation of 1,8-dioxo-octahydroxanthene derivatives by recyclable cobalt-incorporated sulfated zirconia ($ZrO_2/SO_{42}-/Co$) nanoparticles, J. Nanoparticle Res. 21 (2019).
[28] J. Ashtarian, R. Heydari, M.T. Maghsoodlou, A. Yazdani-Elah-Abadi, Bronsted Acidic Ionic Liquids (BAILs)-Catalyzed Synthesis of 1,8-Dioxo-Octahydroxanthene and 2,2′-Arylmethylene Bis(3-Hydroxy-5,5-Dimethyl-2-Cyclohexene-1-One) Derivatives Under Eco-Friendly Conditions, Iran. J. Sci. Technol. Trans. A Sci. 44 (2020) 51–64.
[29] S. Naderi, R. Sandaroos, S. Peiman, B. Maleki, Novel crowned cobalt (II) complex containing an ionic liquid: A green and efficient catalyst for the one-pot synthesis of chromene and xanthene derivatives starting from benzylic alcohols, J. Phys. Chem. Solids. 180 (2023) 111459.
[30] B. Maleki, S. Barzegar, Z. Sepehr, M. Kermanian, R. Tayebee, A novel polymeric catalyst for the one-pot synthesis of xanthene derivatives under solvent-free conditions, J. Iran. Chem. Soc. 9 (2012) 757–765.
[31] B. Maleki, A. Davoodi, M.V. Azghandi, M. Baghayeri, E. Akbarzadeh, H. Veisi, S.S. Ashrafi, M. Raei, Facile synthesis and investigation of 1,8-dioxooctahydroxanthene derivatives as corrosion inhibitors for mild steel in hydrochloric acid solution, New J. Chem. 40 (2016) 1278–1286.
[32] S. Kanagesan, M. Hashim, S.A.B. Aziz, I. Ismail, S. Tamilselvan, N.B. Alitheen, M.K. Swamy, B.P. Chandra Rao, Evaluation of antioxidant and cytotoxicity activities of copper ferrite ($CuFe_2O_4$) and zinc ferrite ($ZnFe_2O_4$) nanoparticles synthesized by sol-gel self-combustion method, Appl. Sci. 6 (2016) 1–13.
[33] S. Krehula, S. Musić, Influence of Mn-dopant on the properties of α-FeOOH particles precipitated in highly alkaline media, J. Alloys Compd. 426 (2006) 327–334.
[34] M. 24 Iacob, Sonochemical synthesis of hematite nanoparticles, Chem. J. Mold. Gen. 10 (2015) 46–51.
[35] F.H. Mulud, N.A. Dahham, I.F. Waheed, Synthesis and Characterization of Copper Ferrite Nanoparticles, IOP Conf. Ser. Mater. Sci. Eng. 928 (2020).
[36] M. Fuentes-Pérez, M. Sotelo-Lerma, J.L. Fuentes-Ríos, E.G. Morales-Espinoza, M. Serrano, M.E. Nicho, Synthesis and study of physicochemical properties of Fe_3O_4@$ZnFe_2O_4$ core/shell nanoparticles, J. Mater. Sci. Mater. Electron. 32 (2021) 16786–16799.

[37] M.A. Zolfigol, R. Ayazi-Nasrabadi, S. Baghery, V. Khakyzadeh, S. Azizian, Applications of a novel nano magnetic catalyst in the synthesis of 1,8-dioxo-octahydroxanthene and dihydropyrano[2,3-c]pyrazole derivatives, J. Mol. Catal. A Chem. 418–419 (2016) 54–67.
[38] M. Hajjami, F. Gholamian, R.H.E. Hudson, A.M. Sanati, FSM-16/AEPC-SO_3H: Synthesis, Characterization and Its Application for the Catalytic Preparation of 1,8-Dioxo-octahydroxanthene and Tetrahydrobenzo[b]pyran Derivatives, Catal. Letters. 149 (2019) 228–247.
[39] H. Naeimi, Z.S. Nazifi, A highly efficient nano-Fe_3O_4 encapsulated-silica particles bearing sulfonic acid groups as a solid acid catalyst for synthesis of 1,8-dioxo-octahydroxanthene derivatives, J. Nanoparticle Res. 15 (2013).
[40] A.N. Dadhania, V.K. Patel, D.K. Raval, Catalyst-free sonochemical synthesis of 1,8-dioxo-octahydroxanthene derivatives in carboxy functionalized ionic liquid, Comptes Rendus Chim. 15 (2012) 378–383.
[41] S. Kamble, G. Rashinkar, A. Kumbhar, R. Salunkhe, Hydrotrope induced synthesis of 1,8-dioxo-octahydroxanthenes in aqueous medium, Green Chem. Lett. Rev. 5 (2012) 101–107.
[42] S. Karhale, M. Patil, G. Rashinkar, V. Helavi, Green and cost effective protocol for the synthesis of 1,8-dioxo-octahydroxanthenes and 1,8-dioxo-decahydroacridines by using sawdust sulphonic acid, Res. Chem. Intermed. 43 (2017) 7073–7086.
[43] A. Ilangovan, S. Malayappasamy, S. Muralidharan, S. Maruthamuthu, A highly efficient green synthesis of 1, 8-dioxo-octahydroxanthenes, Chem. Cent. J. 5 (2011) 2–7.
[44] M. Salami, A. Ezabadi, A caffeine-based ionic liquid as a novel and eco-friendly catalyst for the synthesis of 1,8-dioxo-octahydroxanthenes under solvent-free conditions, Res. Chem. Intermed. 45 (2019) 3673–3686.
[45] S.S. Kahandal, A.S. Burange, S.R. Kale, P. Prinsen, R. Luque, R. V. Jayaram, An efficient route to 1,8-dioxo-octahydroxanthenes and -decahydroacridines using a sulfated zirconia catalyst, Catal. Commun. 97 (2017) 138–145.
[46] H.N. Karade, M. Sathe, M.P. Kaushik, An efficient synthesis of 1,8-dioxo-octahydroxanthenes using tetrabutylammonium hydrogen sulfate, Arkivoc. 2007 (2007) 252–258.
[47] Y. Girish, K. Sharathkumar, K. Prashantha, S. Rangappa, M. Sudhanva, Significance of antioxidants and methods to evaluate their potency, Mater. Chem. Horizons, 2(2) (2023) 93-112.